JOURNAL OF MATERIALS SCIENCE **40** (2005) 1643–1646

Melting behavior and origin of strain in ball-milled nanocrystalline Al powders

Á. RÉVÉSZ
Department of General Physics, Eötvös University, Budapest, H-1518, P.O.B. 32, Budapest, Hungary
E-mail: reveszadam@ludens.elte.hu

Ball-milled aluminum powders have been investigated by differential scanning calorimetry and high resolution X-ray line profile analysis. Ball-milling was carried out for different milling times ranging from 45 min to 32 days. The milling time dependence of the average grain-size and of the density of lattice defects, mainly dislocations, were determined by the modified Williamson-Hall and Warren-Averbach procedures based on the dislocation model of mean square strain. Characteristic grain sizes of ball-milled Al-powders decreases with increasing milling time and simultaneously, the grain-size distribution becomes sharper.

Calorimetric measurements indicated the decrease of the melting point, T_m with increasing milling time. The melting point depression was found to be proportional to inverse grain size.

The strain accumulated in the powder particles is mainly caused by intergrain dislocations.

1. Introduction

Melting behavior is a phenomenon widely studied in materials research, but it is still far from being completely understood [1]. During recent decades the melting behavior of fine particles has been extensively studied. Experimental results have revealed that the melting point, T_m of fine particles exhibits a strong dependence on their sizes [2, 3] and on the interface structure [4].

Ball-milled pure Al powder represents ideal model material for studying melting phenomenon of small particles because during the milling process oxygen penetrates the Al-powder particles by enhanced diffusion along the nanograin boundaries forming a very thin oxide layer around the Al grains. Since the melting point of Al_2O_3 is much higher than that of Al, the individual grains isolated by the oxide layer on the grain boundaries, melt independently. In this paper the influence of the grain size on the melting point and the origin of strain accumulated in nanocrystalline Al-powders will be discussed.

2. Experimental procedures

High purity Al powder (Aldrich, 99.9%, 200 mesh) was ball-milled in a vibratory mill using a hardened stainless steel ball with a diameter of 6 cm. The process was carried out in air with the addition of hexane of approximately 5 ml for different milling times: 45 min, 1.5 h, 3 h, 6 h, 12 h, 24 h, 2 days, 4 days, 8 days, 16 days, 32 days. Each ball-milling procedure was carried out without interruption with a new dose of initial powder of about 1 gram. The contamination from the milling media was monitored by ICP-AES (Inductively coupled plasma-atomic emission spectrometry) method. The Fe contamination of the powder ball-milled for the longest duration (32 days) was 0.3 wt%, hence contamination effects from the ball-mill are negligible.

A Perkin-Elmer differential scanning calorimeter (DSC) was applied to study the variation of the melting point, T_m, as a function of milling time. The DSC curves were carried out at a heating rate of 2 $Kmin^{-1}$ in the temperature range of 910–950 K. Each measurement was immediately followed by a second run in order to investigate the variation of the melting point. The melting temperatures were typically reproducible within several tenths of degrees. All measurements were carried out in a high purity Ar flux. The temperature and the energy were calibrated by measuring the melting thermogram of pure Al and In.

The Al-diffraction peak profiles were measured by a spatial high resolution double crystal diffractometer with negligible instrumental peak broadening. A Nonius 591, fine focus, Co rotating anode X-ray source has been combined with a sagittaly curved Ge monochromator oriented for the symmetrical 440 reflection. The diffracted intensity has been recorded by a linear position sensitive detector (Braun, Munich, OED-50).

3. Results and discussion

The Al-peak profiles were evaluated for the average grain size and the dislocation density by the methods of the *modified* Williamson-Hall plot and the *modified* Warren-Averbach analysis. In these procedures the anisotropic contrast and the strain effects of dislocations on peak broadening have been considered. In the

modified Williamson-Hall plot the total line broadening can be expressed by the following equation [5–7]:

$$\Delta K = 0.9/\langle D\rangle_{\mathrm{vol}} + (\pi A b^2/2)^{1/2}\rho^{1/2}(K\bar{C}^{1/2}) + O(K^2\bar{C}) \quad (1)$$

where ΔK is the full width at half maximum (FWHM) in nm^{-1} units, $K = 2\sin\theta/\lambda$ and $\Delta K = 2\cos\theta(\Delta\theta)/\lambda$, where θ and λ are the diffraction angle and the wavelength of X-rays, respectively. $\langle D\rangle_{\mathrm{vol}}$ is the volume averaged grain size, A is constant depending on the effective outer cut-off radius of dislocations and $b\rho$ and $\bar{C}$ are the Burgers-vector, the dislocation density and the average contrast factor of the dislocations, respectively. For the numerical evaluation of the $\bar{C}$ factors, see ref [8]. The calculated values of $\bar{C}$ are as follows for five different reflections: (111): 0.1096; (200): 0.1930; (220): 0.1298; (311): 0.1533; (222): 0.1096. The *modified* Warren-Averbach method can be written as [5–7]:

$$\ln A(L) \cong \ln A_{\mathrm{L}}^{\mathrm{S}} - \rho(\pi b^2/2)L^2\ln(R_{\mathrm{e}}/L)(K^2\bar{C}) + O(K^4\bar{C}^2) \quad (2)$$

where $A(L)$ are the real part of the Fourier coefficients of the intensity distribution of diffraction profiles and R_{e} is the effective outer cut off radius of dislocations. The Fourier length, L can be expressed as $L = na_3$, where n are integers and a_3 is the unit of the Fourier length in the direction of the diffraction vector. The detailed line-profile analysis corresponding to the ball-milled Al-powders has been published elsewhere [9].

The area averaged grain size, $\langle L\rangle_{\mathrm{area}}$, which is often termed as 'column length', can be obtained from the initial slope of $A_{\mathrm{L}}^{\mathrm{S}}$ vs L [10]:

$$\langle L\rangle_{\mathrm{area}} = -A_0^{\mathrm{S}}/\left(\frac{\mathrm{d}A^{\mathrm{S}}}{\mathrm{d}L}\right)_{\mathrm{L}\to 0}. \quad (3)$$

A volume averaged column length, $\langle L\rangle_{\mathrm{vol}}$, can be obtained by integrating the $A_{\mathrm{L}}^{\mathrm{S}}$ vs. L function:

$$\langle L\rangle_{\mathrm{vol}} = 2\int_0^{\infty} A_{\mathrm{L}}^{\mathrm{S}}\mathrm{d}L. \quad (4)$$

It has to be emphasized that the size quantities primarily resulting from the Fourier analysis of the line profiles are column lengths which, in general, are not identical with particle size, thereby 'column' means a column of lattice cells in the crystallite perpendicular to the diffracting lattice planes.

Fig. 1 shows the variation of the characteristic sizes, $\langle D\rangle_{\mathrm{vol}}$, $\langle L\rangle_{\mathrm{area}}$ and $\langle L\rangle_{\mathrm{vol}}$ as a function of the milling time. As it can be seen, all three grain-size values decrease rapidly at the initial stage of ball-milling up to few days, and afterwards the rate of the grain refinement continuously decreases reaching a minimum value of $\langle D\rangle_{\mathrm{vol}} = 38$ nm, $\langle L\rangle_{\mathrm{area}} = 26$ nm and $\langle L\rangle_{\mathrm{vol}} = 36$ nm after 32 days of ball-milling. These values are in good agreement with TEM observations on ball-milled Al-powders [11, 12]. The ratio $\langle L\rangle_{\mathrm{vol}}/\langle L\rangle_{\mathrm{area}}$ varies between 1.4 and 1.75 for all milling times which interval coincides fairly with results on ball-milled nanocrystalline Fe powders [13]. On the other hand, the dislocation density, ρ, shows a continuous increase from 2×10^{14} m^{-2} (unmilled state) up to 40×10^{14} m^{-2} after 32 days of ball-milling, however, a slight tendency of saturation can be observed (see also Fig. 1).

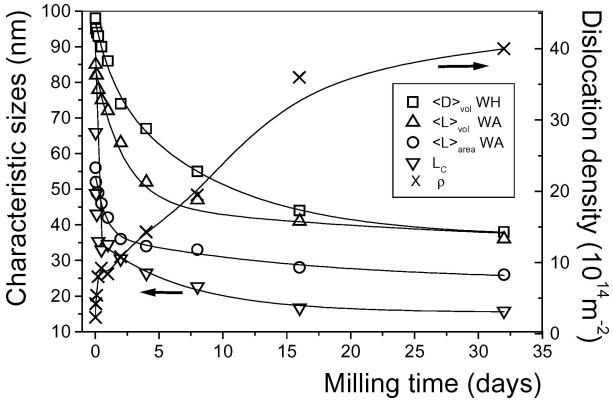

Figure 1 Characteristic sizes and dislocation density as a function of milling time. The values were obtained by the modified Willimason-Hall and Warren-Averbach procedures.

The average dislocation distance, $L_{\mathrm{C}} = \rho^{-1/2}$, shows a monotonous decrease with prolonged milling time. For milling times longer than 6 hours the smallest characteristic size ($\langle L\rangle_{\mathrm{area}}$) is only by a factor of 1.5 larger than the average dislocation distance, indicating that the individual nanograins contain just a few number of dislocations.

The dislocation density varies inversely with the volume averaged grain size for prolonged milling times as shown in Fig. 2. Similar relationship was observed in the behavior of rms lattice strain vs. inverse grain size in the case of nanocrystalline Fe powders [14, 15]. Tian and Atzmon interpreted this phenomenon as a result of two independent effects. The term independent of the grain-size represents the strain resulting from the defects in the grain interior, and the size-dependent term is proportional to the specific grain boundary area and represents the strain resulting from grain boundaries.

The average dislocation distance was found to exhibit a drastic decrease at larger grain sizes, indicating that at the early stages of ball-milling the intensity

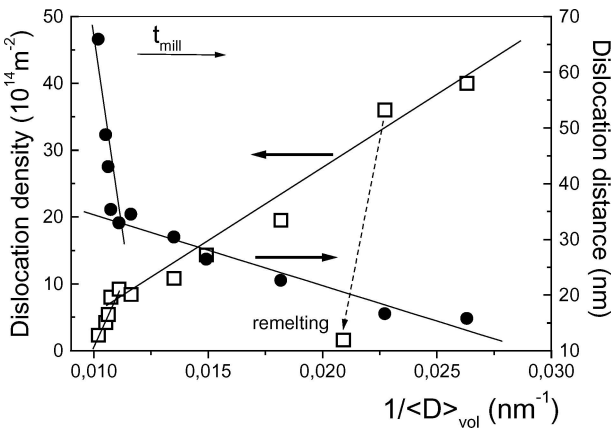

Figure 2 Dislocation density and average dislocation disstance as a function of $1/\langle D\rangle_{\mathrm{vol}}$.

of the dislocation production is much higher than the rate of the grain-size refinment. At prolonged milling times (above 24 h) the decrease of the dislocation distance vs. inverse grain size is reduced, corresponding to simultanous occurance of dislocation production and grain-size refinment.

During the milling process it is assumed that the crystallites are spherical and have a log-normal size distribution:

$$g(L) = \frac{1}{\sqrt{2\pi} L \ln \sigma} \exp\left(-\frac{(\ln(L/D_0))^2}{2(\ln \sigma)^2}\right) \quad (5)$$

where D_0 is the median and σ is the variance of the distribution, respectively. $g(L)$ is normalized as $\int g(L)\,dL = 1$. The two parameters describing the lognormal size distribution can be expressed from the following two equations:

$$\langle L\rangle_{\text{vol}} = \frac{3}{4} D_0 \exp\left(\frac{7}{2}\ln^2\sigma\right) \quad \text{and}$$

$$\langle L\rangle_{\text{area}} = \frac{2}{3} D_0 \exp\left(\frac{5}{2}\ln^2\sigma\right) \quad (6)$$

[16]. The histograms show that with increasing milling time the distribution becomes narrower and shifts towards smaller values (see Fig. 3), indicating that grain-size refinement is accompanied by a more uniform grain-size distribution. Similar behavior was found in ball-milled nanocrystalline iron [13].

In the case of the sample milled for 32 days, the three characteristic sizes are marked on the histogram. $\langle D\rangle_{\text{vol}}$ and $\langle L\rangle_{\text{vol}}$ lay on the right side tail of the distribution function, while $\langle L\rangle_{\text{area}}$ coincides fairly with the maximum of the distribution. This deviation can be explained by the fact that the parameters of the lognormal distribution function are based on the shape of the grains. The distribution functions investigated here are assumed to have just spherical grains, which obviously doesn't fulfill, at least, at the early stages of ball-milling.

The melting thermograms of the nanocrystalline Al-powders exhibit one endothermic peak which is shifted to lower temperature with increasing milling time [9].

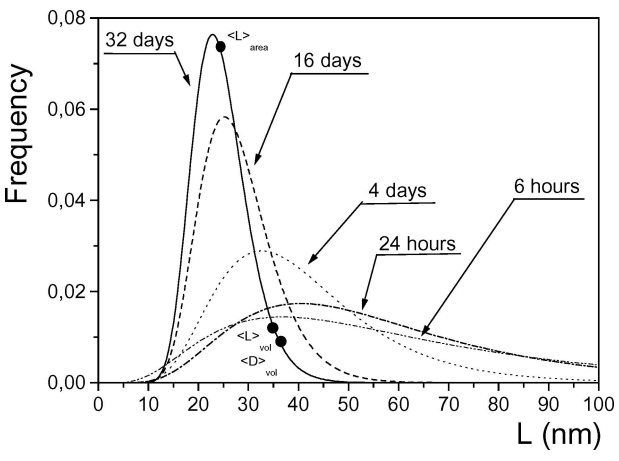

Figure 3 Calculated histograms of grain-sizes in nanocrystalline Al-powders for some selected milling times.

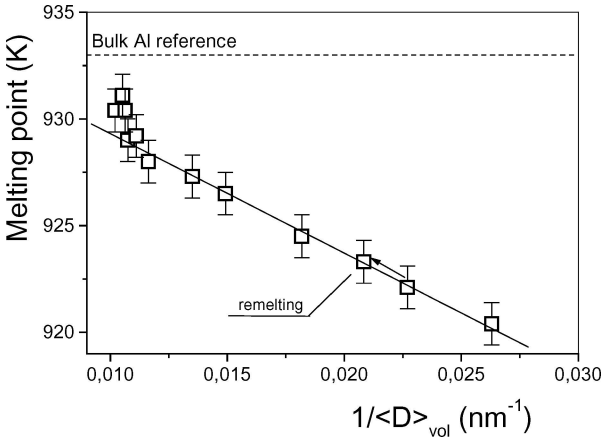

Figure 4 Melting point, T_{m} as a function of the inverse grain size. The dotted line represents the melting temperature of bulk Al.

The melting point was determined as the intercept of the calorimetric baseline and the straight line fitted to the leading edge of the endothermal peak. Remelting the samples leads only a very moderate increase in the melting temperature, but remains far from the bulk value. The melting point depression of ball-milled nanocrystalline materials can be affected by several factors, such as the impurities resulting from the milling media and atmosphere. However, ICP-AES analysis revealed that the Fe contamination in the Al powder milled even for 32 days is negligible. Furthermore neither iron, nor oxygen or nitrogen can lower T_{m} according to the equilibrium phase diagrams [17].

Classical thermodynamic arguments [1, 3] describe the melting point (T_{m}) depression of an ensemble of fine particles as

$$\frac{T_{\text{m}}}{T_0} = 1 - \left(\frac{6(\sigma_{\text{SM}} - \sigma_{\text{LM}})}{< D >_{\text{vol}} L\rho_M}\right) \quad (7)$$

where T_0 is the melting point, L is the enthalpy of fusion, ρ_{M} is the average density of the liquid and solid Al [$\rho = (\rho_{\text{L}} + \rho_{\text{S}})/2$] and σ_{SM} and σ_{LM} denote the surface energy per unit area of the solid Al-solid Al_3O_2 and the liquid Al-solid Al_3O_2 interfaces, respectively. Fig. 4 confirms that the inverse grain-size dependence predicted by the Couchman-Jesser model is experimentally verified, however, some deviation from the fitted straight line can be observed in the early stages of ball-milling. The deviation at large grain-sizes (low milling times up to 12 h) can be attributed to the different particle shapes and to the wide initial grain-size distribution containing a large number of grains far from the maximum of the distribution (see Fig. 3). By extrapolating the fitted line to the case of infinite crystal ($1/\langle D\rangle_{\text{vol}} = 0$), the obtained value (936 K) coincides satisfactorily with the melting temperature of bulk Al. From the slope of fitted straight line (675 nmK) with available data of L, ρ_{M} and T_0 for Al [17], $\sigma_{\text{SM}} - \sigma_{\text{LM}}$ can be obtained as 0.12 J/m^2.

The point corresponding to the remelted sample still fits the same line indicating that after freezing the magnitude of $\sigma_{\text{SM}} - \sigma_{\text{LM}}$ remains unchanged. This suggests that the grain boundary structure of the Al particles

(within the Al_2O_3 shells) formed after melting and refreezing is practically unchanged compared to the as-milled samples. The X-ray line profile analysis results revealed that the dislocation density in the melted and subsequently refrozen samples is nearly equal to zero (see the dashed arrow in Fig. 2) which indicates that strain broadening accumulated in the ball-milled samples is mainly due intergrain dislocations. Therefore, the effect of Al/Al_2O_3 interfaces and triple junctions in line broadening is negligible.

4. Conclusions

In this paper it was shown that the microstructure of nanocrystalline Al powders undergoes a significant change during ball-milling. The different characteristic grain sizes obtained from high resolution X-ray line profile analysis decrease with increasing milling time and simultaneously, the grain size distribution becomes sharper.

The melting point depression of ball-milled Al-powders followed the inverse grain-size relationship. Because of the oxide film on the grain boundaries, melting and refreezing of the Al particles does not change the grain boundary structure. The experimental results demonstrate clearly that the strain accumulated in the ball-milled Al powders is mainly caused by dislocations inside the grains, the role of the grain boundaries and triple junctions in line broadening is negligible.

Acknowledgements

This work has been supported by the Hungarian Scientific Research Fund (OTKA) under grant No. T043247 and T046990. Special thanks to Prof. Gy. Zarai and A. Varga for the chemical analysis.

References

1. G. L. ALLEN, W. W. GILE and W. A. JESSER, *Acta Met.* **28** (1980) 1695.
2. P. BUFFAT and J. P. BOREL, *Phys. Rev. A* **13** (1976) 2287.
3. P. R. CHOUCHMAN and W. A. JESSER, *Phil. Mag. Lett.* **35** (1977) 223.
4. H. W. SHENG, Z. Q. HU and K. LU, *Nanostruct. Mat.* **9** (1997) 661.
5. T. UNGÁR and A. BORBÉLY, *Appl. Phys. Lett.* **69** (1996) 3173.
6. Á. RÉVÉSZ, T. UNGÁR, A. BORBÉLY and J. LENDVAI, *Nanostruct. Mat.* **7** (1996) 779.
7. T. UNGÁR, G. RIBÁRIK, J. GUBICZA and A. BORBÉLY, *J. Appl. Cryst.* **34** (2001) 298.
8. T. UNGÁR, I. DRAGOMIR, Á. RÉVÉSZ and A. BORBÉLY, *ibid.* **32** (1999) 992.
9. Á. RÉVÉSZ, J. LENDVAI and T. UNGÁR, *Mat. Sci. Forum* **343–346** (2000) 326.
10. B. E. WARREN, "X-ray Diffraction" (1968) Chapt. 13.
11. J. ECKERT, J. C. HOLZER, C. C. AHN, Z. FU and W. L. JOHNSON, *Nanostruct. Mat.* **2** (1993) 407.
12. F. ZHOU, J. LEE and E. J. LAVERNIA, *Scripta Mater.* **44** (2001) 2013.
13. H. H. TIAN and M. ATZMON, *Phil. Mag. A.* **79** (1999) 1769.
14. *Idem.*, *Acta Mater.* **47** (1999) 1255.
15. T. R. MALOW and C. C. KOCH, *ibid.* **45** (1997) 2177.
16. C. R. KRILL and R. BIRRINGER, *Phil. Mag. A* **77** (1998) 621.
17. L. F. MONDOLFO, "Aluminium Alloys: Structure and Properties" (Butterworth & Co. Publisher, 1976).
18. D. R. LIDE, "Handbook of Chemistry and Physics," 71st edn. (CRC Press, 1990–1991).

Received 22 January
and accepted 8 November 2004